Macroscopic quantum coherence in spinor condensates confined in an anisotropic potential

Yixiao Huang,[1,4] Yunbo Zhang,[2] Rong Lü,[3] Xiaoguang Wang,[1] and Su Yi[4,*]

[1]*Department of Physics, Zhejiang Institute of Modern Physics, Zhejiang University, Hangzhou 310027, China*

[2]*Institute of Theoretical Physics, Shanxi University, Taiyuan 030006, China*

[3]*Department of Physics, Tsinghua University, Beijing 100084, China*

[4]*State Key Laboratory of Theoretical Physics, Institute of Theoretical Physics, Chinese Academy of Sciences, P.O. Box 2735, Beijing 100190, China*

(Received 17 June 2012; published 25 October 2012)

We investigate the macroscopic quantum spin coherence of a spinor condensate confined in an anisotropic potential. Under the single-mode approximation, we show that a spin-1 Rb condensate can be modeled as a biaxial quantum magnet. A direct consequence of the biaxial anisotropy is that the tunneling splitting oscillates as a function of the external magnetic field applied along the hard axis. We also propose an experimental scheme to detect the oscillatory behavior of the tunneling splitting by employing the Landau-Zener tunneling.

DOI: 10.1103/PhysRevA.86.043625 PACS number(s): 03.75.Mn, 75.45.+j

I. INTRODUCTION

Tunneling of a macroscopic variable into a classically forbidden region provides one of the most striking manifestations of quantum mechanics [1]. The model of quantum tunneling often involves a particle moving in a multistable potential. Quantum mechanically, there is a finite probability for the particle to tunnel through the barrier and escape from a metastable state to an absolutely stable one, which is often referred to as macroscopic quantum tunneling (MQT). In a symmetric double-well, the particle tunnels through the barrier to oscillate back and forth between the degenerate states, known as macroscopic quantum coherence (MQC). Quantum tunneling removes the degeneracy of the ground states, resulting in a tunneling splitting between the true ground state and the first excited state.

Because of its small size and precise characterizability, the single-molecule nanomagnet represents an ideal platform for demonstrating the MQT and MQC of the spin [2–6]. For such a system, MQT consists of tunneling of the magnetization out of the metastable easy directions in the presence of an external field, which was experimentally observed as a series of steps in the hysteresis loops in Mn_{12}-acetate and Fe_8 molecules at low temperatures [7–10]. MQC in spin systems represents the resonance between two equivalent easy directions. Of particular interest, in the presence of a general biaxial anisotropy, the spin has two preferred tunneling paths via the medium axis when the external field is applied along the hard direction. As a result, constructive and destructive interferences give rise to oscillatory tunneling splitting [11,12], which is direct evidence of the topological quantum interference of two tunnel paths of opposite windings in magnetic molecular clusters [13].

In the context of ultracold atomic gases, the MQC problem was previously studied for a spinor condensate trapped in a double-well potential, where the magnetic dipole-dipole interaction (MDDI) between the condensates confined in different wells induces a uniaxial anisotropy, with the easy axis being along the direction connecting two potential wells [14]. In fact, even in a single axially symmetric trap, a dipolar spinor condensate can be treated as a uniaxial quantum magnet [15], whose magnetic properties, spin squeezing, magnetization steps, macroscopic entanglement generation, and MQC were studied [16,17]. However, for a uniaxial quantum magnet, the tunneling splitting of the model is a monotonically increasing function of the transverse field strength [14]. The possibility of obtaining oscillatory tunneling splitting in ultracold atomic gases was explored by considering a condensate coupled dispersively with an ultrahigh-finesse optical cavity [18].

In the present work, we investigate the MQC of a spin-1 Rb condensate confined in a three-dimensional anisotropic harmonic oscillator potential. Under the single-mode approximation (SMA), we show that the interplay of the MDDI and the anisotropic trap results in a biaxial quantum magnet whose magnetic structure can be approximately specified by the geometry of the trapping potential. Subsequently, we study the MQC of the condensate by applying an external magnetic field along the hard axis. We show that the tunneling splitting of our system oscillates as a function of the field strength, similarly to the molecular magnet,. Finally, utilizing the Landau-Zener transition, we propose an experimental scheme to detect MQC in spin-1 condensates by measuring the atom number in each spin component.

This paper is organized as follows. In Sec. II, we derive the Hamiltonian of the system under the SMA. In Sec. III, the magnetic structure of the system is explored. Section IV is devoted to the properties of MQC and its experimental detection. Finally, we conclude in Sec. V

II. MODEL

We consider a trapped gas of N spin $F = 1$ Rb atoms subjected to an external magnetic field $\mathbf{B}$. Atoms interact via s-wave collisions and the MDDI. In the second quantized form,

*syi@itp.ac.cn

the total Hamiltonian of the system reads [15]

$$\mathcal{H} = \int d\mathbf{r}\hat{\psi}^\dagger_\alpha(\mathbf{r})\left[\left(-\frac{\hbar^2\nabla^2}{2M} + V_{\rm ext}(\mathbf{r})\right)\delta_{\alpha\beta} - g_F\mu_B\mathbf{B}\cdot\mathbf{F}_{\alpha\beta}\right]\hat{\psi}_\beta(\mathbf{r}) + \frac{c_0}{2}\int d\mathbf{r}\hat{\psi}^\dagger_\alpha(\mathbf{r})\hat{\psi}^\dagger_\beta(\mathbf{r})\hat{\psi}_\alpha(\mathbf{r})\hat{\psi}_\beta(\mathbf{r}) + \frac{c_2}{2}\int d\mathbf{r}\hat{\psi}^\dagger_\alpha(\mathbf{r})\hat{\psi}^\dagger_{\alpha'}(\mathbf{r})\mathbf{F}_{\alpha\beta}\cdot\mathbf{F}_{\alpha'\beta'}\hat{\psi}_\beta(\mathbf{r})\hat{\psi}_{\beta'}(\mathbf{r}) + \frac{c_d}{2}\int\frac{d\mathbf{r}d\mathbf{r}'}{|\mathbf{r}-\mathbf{r}'|^3}\left[\hat{\psi}^\dagger_\alpha(\mathbf{r})\hat{\psi}^\dagger_{\alpha'}(\mathbf{r}')\mathbf{F}_{\alpha\beta}\cdot\mathbf{F}_{\alpha'\beta'}\hat{\psi}_\beta(\mathbf{r})\hat{\psi}_{\beta'}(\mathbf{r}') - 3\hat{\psi}^\dagger_\alpha(\mathbf{r})\hat{\psi}^\dagger_{\alpha'}(\mathbf{r}')(\mathbf{F}_{\alpha\beta}\cdot\mathbf{e})(\mathbf{F}_{\alpha'\beta'}\cdot\mathbf{e})\hat{\psi}_\beta(\mathbf{r})\hat{\psi}_{\beta'}(\mathbf{r}')\right], \quad (1)$$

where $\hat{\psi}_\alpha$ is the field operator for the $m_F = \alpha$ spin state, $V_{\rm ext}$ is the anisotropic confining potential, $\mathbf{F}$ is the angular momentum operator, g_F is the Landé g factor, and μ_B is the Bohr magneton. The spin-independent and spin-exchange s-wave collsions are characterized by $c_0 = 4\pi\hbar^2(a_0+2a_2)/(3M)$ and $c_2 = 4\pi\hbar^2(a_2-a_0)/(3M)$, respectively, with $a_{f=0,2}$ being the scattering length of two spin-1 atoms in the combined symmetric channel of the total spin f [19,20]. In particular, we have $c_2 < 0$ for Rb atoms, indicating that the spin-exchange interaction is ferromagnetic. The strength of the MDDI is $c_d = \mu_0\mu_B^2 g_F^2/(4\pi)$, with μ_0 being the vacuum permeability.

To proceed further, we adopt the SMA, which assumes that atoms in different spin states share a common spatial mode function $\phi(\mathbf{r})$. The field operators can then be decomposed into [21]

$$\hat{\psi}_\alpha(\mathbf{r}) \simeq \phi(\mathbf{r})\hat{a}_\alpha, \quad (2)$$

where $\hat{a}_\alpha$ is the annihilation operator of the spin component α. The validity of the SMA can be justified by noting that $c_0 \gg |c_2|$ and $c_d \simeq 0.1|c_2|$ for Rb atoms [22]. By substituting Eq. (2) into Eq. (1) and dropping the constant terms, the total Hamiltonian reduces to

$$\mathcal{H} = (c_2' - c_d')\hat{\mathbf{S}}^2 + 3c_d'\hat{S}_z^2 - 3c_d''\left(\hat{S}_x^2 - \hat{S}_y^2\right) - g_F\mu_B\mathbf{B}\cdot\hat{\mathbf{S}} + 3c_d'\hat{a}_0^\dagger\hat{a}_0 + 3c_d''(\hat{a}_{-1}^\dagger\hat{a}_1 + \hat{a}_1^\dagger\hat{a}_{-1}), \quad (3)$$

where $\hat{\mathbf{S}} = \sum_{\alpha\beta}\hat{a}^\dagger_\alpha\mathbf{F}_{\alpha\beta}a_\beta$ is the total many-body angular momentum operator and $\hat{S}_\eta$ $(\eta = x,y,z)$ is its projection along the η axis, $c_2' = (c_2/2)\int d\mathbf{r}|\phi(\mathbf{r})|^4$ is the strength of spin-exchange interaction, and the strength of the MDDI is characterized by two parameters, $c_d' = (c_d/4)\int d\mathbf{r}\,d\mathbf{r}'|\phi(\mathbf{r})|^2|\phi(\mathbf{r}')|^2|\mathbf{r}-\mathbf{r}'|^{-3}(1-3\cos^2\vartheta)$ and $c_d'' = (c_d/4)\int d\mathbf{r}d\mathbf{r}'|\phi(\mathbf{r})|^2|\phi(\mathbf{r}')|^2|\mathbf{r}-\mathbf{r}'|^{-3}\sin^2\vartheta\, e^{2i\varphi}$, with ϑ and φ being the polar and azimuthal angles of the vector $\mathbf{r}-\mathbf{r}'$, respectively. It can be shown that $c_d'' = 0$ if the mode function $\phi(\mathbf{r})$ possesses an axial symmetry [15]. One should note that the last line in Eq. (3) originates from the commutation relations between the bosonic operators.

It is convenient to rescale the Hamiltonian, Eq. (3), by using $|c_2'|$ as the energy unit, which yields the dimensionless Hamiltonian

$$\mathcal{H} = \mathcal{H}_0 + \mathcal{H}', \quad (4)$$

$$\mathcal{H}_0 = -\frac{3+D}{3}\hat{\mathbf{S}}^2 - D\hat{S}_z^2 + E\left(\hat{S}_x^2 - \hat{S}_y^2\right) - \mathbf{H}\cdot\hat{\mathbf{S}}, \quad (5)$$

$$\mathcal{H}' = -D\hat{a}_0^\dagger\hat{a}_0 - E(\hat{a}_{-1}^\dagger\hat{a}_1 + \hat{a}_1^\dagger\hat{a}_{-1}), \quad (6)$$

where $D = -3c_d'/|c_2'|$ and $E = -3c_d''/|c_2'|$ are, respectively, the axial and transverse anisotropy constants and $\mathbf{H} = g_F\mu_B\mathbf{B}/|c_2'|$ is the strength of the external magnetic field. Apparently, the Hamiltonian, Eq. (5), describes a biaxial quantum magnet. More specifically, we assume that the mode function is a Gaussian, $\phi(\mathbf{r}) = \pi^{-3/4}(q_xq_yq_z)^{-1/2}e^{-\sum_{\eta=x,y,z}\eta^2/(2q_\eta^2)}$, with q_η being the width of the condensate along the η direction. It can be shown that

$$D(\kappa_x,\kappa_y) = -\frac{4\pi c_d}{|c_2|}\kappa_x\kappa_y\int_0^\infty dt\, te^{-(\kappa_x^2+\kappa_y^2)t^2/2} \times I_0\left(\frac{1}{2}(\kappa_x^2-\kappa_y^2)t^2\right)[2-3\sqrt{\pi}\,te^{t^2}\mathrm{erfc}(t)],$$

$$E(\kappa_x,\kappa_y) = -\frac{4\pi^{3/2}c_d}{|c_2|}\kappa_x\kappa_y\int_0^\infty dt\, t^2e^{-(\kappa_x^2+\kappa_y^2)t^2/2} \times I_1\left(\frac{1}{2}(\kappa_x^2-\kappa_y^2)t^2\right)e^{t^2}\mathrm{erfc}(t),$$

where $(\kappa_x,\kappa_y) \equiv (q_x/q_z, q_y/q_z)$ characterizes the shape of the condensate, $I_{0,1}(\cdot)$ is the modified Bessel functions of the first kind, and $\mathrm{erfc}(\cdot)$ is the complementary error function. Figure 1 shows the values of $D(\kappa_x,\kappa_y)$ and $E(\kappa_x,\kappa_y)$ for a Rb condensate. In particular, $E(\kappa_x,\kappa_y) = 0$ when $\kappa_x = \kappa_y$, and the condensate becomes a uniaxial magnet [15,16].

III. MAGNETIC STRUCTURE

The ground-state wave function of the system can be found by numerically diagonalizing the Hamiltonian, Eq. (4), in the basis formed by the common eigenstates of $\hat{\mathbf{S}}^2$ and $\hat{S}_z$, i.e., $\{|S,m\rangle\}$, which satisfy

$$\hat{\mathbf{S}}^2|S,m\rangle = S(S+1)|S,m\rangle,$$
$$\hat{S}_z|S,m\rangle = m|S,m\rangle,$$

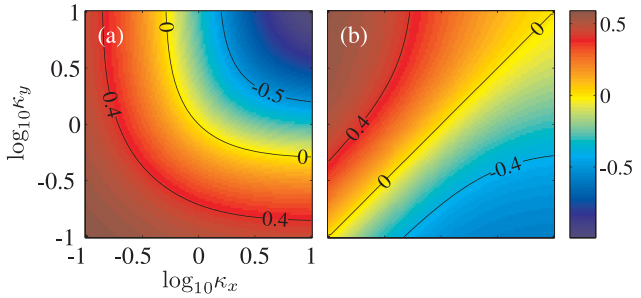

FIG. 1. (Color online) Anisotropic constants (a) $D(\kappa_x,\kappa_y)$ and (b) $E(\kappa_x,\kappa_y)$ for Rb condensates.

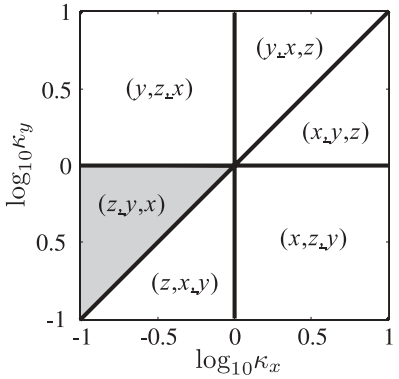

FIG. 2. Magnetic structure of a Rb condensate on the parameter (κ_x,κ_y) plane in terms of (easy, medium, hard) axes in the absence of magnetic field. Solid lines correspond to uniaxial magnets. With the help of Eq. (8), the easy (hard) axis corresponds to the direction of minimum (maximum) energy, while the medium axis direction is associated with a saddle point in the energy.

where the total spin, $S = N, N-2, \ldots$, is a non-negative integer and $m = -S, -S+1, \ldots, S$ is the projection of the spin along the z axis [21,23]. For the parameter regime covering $0.1 \leqslant \kappa_{x,y} \leqslant 10$ and under an arbitrary magnetic field, we find that $\langle \hat{\mathbf{S}}^2 \rangle \simeq N(N+1)$ for $N \geqslant 5$, which implies that the condensate with a sufficiently large number of atoms always remains in a ferromagnetic state with total spin $S \simeq N$. In addition, it is also found that the contribution of $\mathcal{H}'$ [Eq. (6)] is negligible. Consequently, we may drop the constant $\mathbf{S}^2$ term in $\mathcal{H}_0$ and the linear term $\mathcal{H}'$ such that Eq. (4) reduces to the familiar biaxial Hamiltonian [12],

$$\mathcal{H}_{\text{eff}} \simeq -D\hat{S}_z^2 + E\left(\hat{S}_x^2 - \hat{S}_y^2\right) - \mathbf{H}\cdot\hat{\mathbf{S}}, \tag{7}$$

for quantum magnet with total spin $S = N$.

In the absence of the external magnetic field, the magnetic properties of the Hamiltonian $\mathcal{H}_{\text{eff}}$ is completely determined by the anisotropy constants D and E: the axial term, $-D\hat{S}_z^2$, splits the degeneracy of the spin states of different m's, whereas the transverse term, $E(\hat{S}_x^2 - \hat{S}_y^2)$, mixes them up. In Fig. 2, we classify the magnetic structure of the system on the (κ_x,κ_y) parameter plane in terms of the easy, medium, and hard axes, which essentially states that the easy (hard) axis corresponds to the direction with the weakest (strongest) trap confinement. Intuitively, the results presented in Fig. 2 can be understood as follows. Without the MDDI, the ground-state energy is degenerate with respect to the orientation of the spin. The MDDI removes this degeneracy by pointing the spin to certain directions. Note that, for two magnetic dipoles, the dipolar interaction is attractive (repulsive) for a head-to-tail (side-by-side) configuration. Therefore, the spins prefer to align along the direction such that the possibility for a head-to-tail configuration is maximized, which is exactly the direction corresponding to the weakest confinement.

IV. MACROSCOPIC QUANTUM COHERENCE

A simple model for studying the MQC problem is a uniaxial magnet with easy-axis anisotropy, which can be realized, for example, by taking $D < 0$ and $E = 0$ in Hamiltonian (4). For ultracold atomic gases, the MQC of this model was previously studied in Refs. [14,17]. Here, without loss of generality, we focus on the MQC of a biaxial magnet with $D > E > 0$, which corresponds to the geometric parameters (κ_x,κ_y) in the shaded region in Fig. 2. The magnetic field is applied along the hard axis, i.e., $\mathbf{H} = H_x\hat{\mathbf{x}}$.

We first consider the classical counterpart of the reduced Hamiltonian, (7), by treating $\hat{\mathbf{S}}$ as a vector of length $|\mathbf{S}| = N$. The total energy then becomes

$$\begin{aligned}\mathcal{E}(\theta,\phi) = &-DN^2\cos^2\theta + EN^2\sin^2\theta\cos 2\phi \\ &- H_x N\sin\theta\cos\phi,\end{aligned} \tag{8}$$

where (θ,ϕ) denotes the direction of $\mathbf{S}$. Apparently, for $H_x < H_x^* \equiv 2N(D+E)$, there exist two degenerate ground states, located at $(\theta_0,0)$ and $(\pi-\theta_0,0)$ with $\sin\theta_0 = H_x/[2N(D+E)]$. When $H_x \geqslant H_x^*$, the double degeneracy is removed such that the system is fully polarized along the x axis by the external field.

Quantum mechanically, the classical degeneracy of the ground states is lifted by quantum tunneling even when $H_x < H_x^*$, which results a tunneling splitting $\Delta\mathcal{E}$ between the true ground state and the first excited state. Of particular interest, with biaxial anisotropy, there exist two tunneling paths with opposite windings on the yz easy-anisotropy plane. Constructive and destructive interferences of quantum spin phases of the different paths cause the tunneling splitting to oscillate with the magnetic field. This phenomenon was first predicted by Garg [11] and was experimentally observed by Wernsdorfer and Sessoli in Mn_{12} molecules [12]. Using the instanton method, the tunneling splitting can be expressed analytically as [11,24]

$$\Delta\mathcal{E}_{\text{in}} = \Delta\varepsilon_0|\cos(\pi\Theta)|, \tag{9}$$

where $\Theta(H_x) = N - H_x/[2\sqrt{2E(D+E)}]$ is the area on the Bloch sphere enclosed by the two instanton paths and $\Delta\varepsilon_0$ is the tunneling splitting under zero external field, which contains the contributions from the classical action and the fluctuations around the instanton paths [11,24]. Surprisingly, quantum tunneling is completely quenched whenever $\Theta = n + 1/2$, with n being an integer. The period of this oscillation is [11]

$$\Delta H_x = 2\sqrt{2E(D+E)}. \tag{10}$$

We want to emphasize that the instanton method is only valid for $H_x < H_x^*$, as it depends on the classical paths of the tunneling.

In Fig. 3, we present the field dependence of the tunneling splitting $\Delta\mathcal{E}$ obtained via the exact numerical diagonalization of the full Hamiltonian, (4), for $N = 10$, $\log_{10}\kappa_x = -0.9$, and $\log_{10}\kappa_y = -0.1$. As a comparison, we also plot $\Delta\mathcal{E}_{\text{in}}$ [Eq. (9)] by adopting the analytic expression of $\Delta\varepsilon_0$ in Ref. [24]. For small H_x, the results obtained from the numerical and the instanton methods are in good agreement, which further confirms that our system is well described by the reduced Hamiltonian. However, a significant discrepancy is observed for the larger external field. It is also found that, by increasing the atom number N, the agreement between the numerical and the instanton methods can be improved.

We now discuss the experimental detection of MQC in spin-1 Rb condensates. Here we adopt a scheme similar to that used in the molecular magnet experiment by utilizing

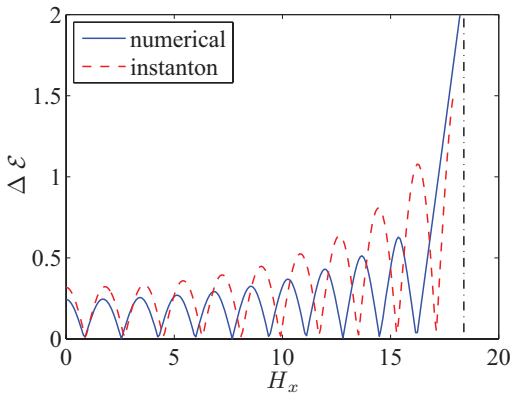

FIG. 3. (Color online) Tunneling splitting as a function of external magnetic field for $\log_{10}\kappa_x = -0.9$, $\log_{10}\kappa_y = -0.1$, and $N = 10$. The vertical dash-dotted line marks the position of the critical field.

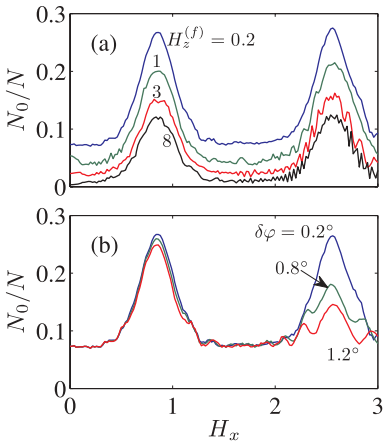

FIG. 4. (Color online) N_0/N as a function of H_x for (a) $\delta\varphi = 0$ with different $H_z^{(f)}$ and (b) $\delta\varphi \neq 0$ with $H_z^{(f)} = 0.2$. Other parameters are $N = 10$, $\log_{10}\kappa_x = -0.9$, $\log_{10}\kappa_y = -0.1$, $v = 10^{-3}$, and $H_z^{(i)} = -8$.

the Landau-Zener transition [12]. More specifically, the experiment can be carried out as follows. In addition to the constant transverse field $H_x\hat{\mathbf{x}}$, we introduce a time-dependent longitudinal magnetic field $H_z(t)\hat{\mathbf{z}}$ which is swept linearly at a constant rate $v > 0$; i.e., $H_z(t) = H_z^{(i)} + vt$ for $t \geqslant 0$, where $H_z^{(i)} < 0$ is the initial field. When the longitudinal field reaches the value $H_z^{(f)} \equiv H_z^{(i)} + vt_f > 0$ at $t = t_f$, one measures the number of atoms N_α in each spin component.

As can be seen from the reduced Hamiltonian, (7), if the initial longitudinal field $H_z^{(i)}$ is sufficiently large, the initial state roughly stays at the $S_z = -N$ level, which anticrosses with the $S_z = N$ level at $H_z = 0$. When the longitudinal field sweeps through this avoided crossing, a Landau-Zener transition occurs. Since the energy gap between the levels $S_z = -N$ and N at the anticrossing is exactly the tunneling splitting $\Delta\mathcal{E}$, which depends on the transverse field, it is expected that N_α will also oscillate as a function of H_x.

The proposed experiment can be simulated by numerically evolving the full Hamiltonian, (4), with the initial state being the ground state under the magnetic field $H_z^{(i)}$. Figure 4(a) shows the typical transverse field dependence of N_0 for various final longitudinal fields $H_z^{(f)}$. As expected, N_0 oscillates as a function of the transverse field strength. The oscillation period is also in very good agreement with that of $\Delta\mathcal{E}$. In addition, with increasing $H_z^{(f)}$, more anticrossings in the energy spectrum of Hamiltonian (4) are swept through. As a result, the oscillation amplitude decreases with $H_z^{(f)}$, and eventually $N_0(H_x)$ will roughly converge to the curve corresponding to $H_z^{(f)} = 8$ as one increases $H_z^{(f)}$ further. Experimentally, it is possible that the transverse field is misaligned such that it forms an angle $\delta\varphi$ to the x axis. In Fig. 4(b), we plot $N_0(H_z)$ for $\delta\varphi \neq 0$. The oscillation remains for small $\delta\varphi$, however, it will disappear for large $\delta\varphi$. Finally, we remark that N_1 and N_{-1} also exhibit oscillatory behavior similar to that of $N_0(H_z)$.

V. CONCLUSION

To conclude, we have studied the MQC of a spin-1 Rb condensate confined in an anisotropic trap. Under the SMA, we have shown that this system can be described as a biaxial quantum magnet. Physically, biaxial anisotropy is induced by the interplay of the MDDI and the anisotropic trap. Subsequently, we showed that the magnetic structure of the system is determined by the geometric parameters of the trapping potential. We have then studied the MQC of the spinor condensate by applying an external magnetic field along the hard axis of the system, it was shown that the tunneling splitting oscillates as a function of the field strength. Finally, we have proposed an experimental scheme to detect MQC by utilizing the Landau-Zener transition.

ACKNOWLEDGMENTS

S.Y. acknowledges support from the NSFC (Grant No. 11025421) and the National 973 program (Grant No. 2012CB922104). X.W. acknowledges support from the NSFC (Grant No. 11025527) and NFRPC (Grant No. 2012CB921602). Y.H. acknowledges support from the NSFC (Grant No. 10935010). Y.Z. acknowledges support from the NSFC (Grant No. 11074153). R.L. acknowledges support from the NSFC (Grant No. 10974112).

[1] A. J. Leggett, S. Chakravarty, A. T. Dorsey, M. P. A. Fisher, A. Garg, and W. Zwerger, Rev. Mod. Phys. **59**, 1 (1987).

[2] L. Gunther and B. Barbara, eds., *Quantum Tunneling of Magnetization—QTMÕ94* (Kluwer, Dordrecht, Netherlands, 1995).

[3] D. Gatteschi, R. Sessoli, and J. Villain, *Molecular Nanomagnets* (Oxford University Press, Oxford, 2006).

[4] E. M. Chudnovsky, *Macroscopic Quantum Tunneling of the Magnetic Moment* (Cambridge University Press, Cambridge, 1998).

[5] J. S. Miller and M. Drillon, eds., *Magnetism: Molecules to Materials III* (Wiley-VCH Verlag, Weinheim, Germany, 2002).
[6] J. R. Friedman and M. P. Sarachik, Annu. Rev. Condens. Matter Phys. **1**, 109 (2010).
[7] J. R. Friedman, M. P. Sarachik, J. Tejada, and R. Ziolo, Phys. Rev. Lett. **76**, 3830 (1996).
[8] J. M. Hernández, X. X. Zhang, F. Luis, J. Bartolomé, J. Tejada, and R. Ziolo, Europhys. Lett. **35**, 301 (1996).
[9] L. Thomas, F. Lionti, R. Ballou, D. Gatteschi, R. Sessoli, and B. Barbara, Nature **383**, 145 (1996).
[10] C. Sangregorio, T. Ohm, C. Paulsen, R. Sessoli, and D. Gatteschi, Phys. Rev. Lett. **78**, 4645 (1997).
[11] A. Garg, Europhys. Lett. **22**, 205 (1993).
[12] W. Wernsdorfer and R. Sessoli, Science **284**, 133 (1999).
[13] D. Loss, D. P. DiVincenzo, and G. Grinstein, Phys. Rev. Lett. **69**, 3232 (1992).
[14] H. Pu, W. P. Zhang, and P. Meystre, Phys. Rev. Lett. **89**, 090401 (2002).
[15] S. Yi, L. You, and H. Pu, Phys. Rev. Lett. **93**, 040403 (2004).
[16] S. Yi and H. Pu, Phys. Rev. A **73**, 023602 (2006).
[17] L. Yang and Y. Zhang, Phys. Rev. A **74**, 043604 (2006).
[18] G. Chen, J.-Q. Liang, and S. Jia, Opt. Express **17**, 19682 (2009).
[19] T.-L. Ho, Phys. Rev. Lett. **81**, 742 (1998).
[20] T. Ohmi and K. Machida, J. Phys. Soc. Jpn. **67**, 1822 (1998).
[21] C. K. Law, H. Pu, and N. P. Bigelow, Phys. Rev. Lett. **81**, 5257 (1998).
[22] S. Yi, Ö. E. Müstecaplıoğlu, C.-P. Sun, and L. You, Phys. Rev. A **66**, 011601(R) (2002); S. Yi and H. Pu, Phys. Rev. Lett. **97**, 020401 (2006).
[23] Y. Wu, Phys. Rev. A **54**, 4534 (1996).
[24] S. P. Kou, J. Q. Liang, Y. B. Zhang, and F. C. Pu, Phys. Rev. B **59**, 11792 (1999).